

Abundance distributions over the surfaces of magnetic ApBp stars: theoretical predictions

G. Alecian^{1*}

¹LUTH, Observatoire de Paris, CNRS, Université Paris Diderot, 5 Place Jules Janssen, F-92190 Meudon, France

Accepted 2015 September 22. Received 2015 September 21; in original form 2015 April 29

ABSTRACT

Recently published empirical abundance maps, obtained through (Zeeman) Doppler mapping (ZDM), do not **currently** agree with the abundance structures predicted by means of numerical models of atomic diffusion in magnetic atmospheres of ApBp stars. In a first step towards the resolution of these discrepancies, we present a state of the art grid of equilibrium abundance stratifications in the atmosphere of a magnetic Ap star with $T_{\text{eff}} = 10000$ K and $\log g = 4.0$. A description of the behaviour of 16 chemical elements including predictions concerning the over- and/or under-abundances over the stellar surface is followed by a discussion of the possible influence of presently neglected physical processes.

Key words: atomic diffusion - stars: abundances - stars: chemically peculiar - magnetic fields - stars : magnetic fields

1 INTRODUCTION

Magnetic ApBp stars are known to exhibit inhomogeneous distributions of chemical elements over their surface. Babcock (1949b) and later Babcock & Burd (1952) observed a variable magnetic field in α^2 CVn which could, as in the case of a number of other magnetic stars (Babcock 1958), be interpreted in terms of the so-called oblique rotator model. Here the magnetic axis of the rotating star is inclined with respect to the rotational axis (Babcock 1949a). Deutsch (1956) speculated that the observed periodic spectral variations and radial velocity variations were in some way related to the magnetic field and worked out a method to map the abundances of various chemical elements. This early work made it clear that there had to be some correlation between the magnetic fields of a number of Ap stars and the abundance anomalies seen in the spectra.

Later on, several studies tried to map the abundances at the surface of these magnetic Ap stars (review by Khokhlova 1994). With spectra of better S/N ratio and with the full Stokes *IQUV* profiles available at high spectral resolution, modern mapping methods allow the simultaneous determination of the magnetic field geometry and the horizontal abundance distributions over the stellar surface (see for instance the study of α^2 CVn by Silvester et al. 2014). Vertical stratifications of chemical elements in the atmospheres of ApBp peculiar stars have also been detected in magnetic ApBp stars (a recent review is given by Ryabchikova 2008).

Bailey et al. (2014) have published evidence for secular variations in the abundances of ApBp stars, and it has also been shown that the pulsation properties of rapidly oscillating Ap (roAp) stars are affected by abundance spots caused by the magnetic field (Freyhammer et al. 2009).

On the theoretical side, atomic diffusion driven by radiative accelerations has been proposed by Michaud (1970) to explain abundance anomalies in Ap star atmospheres. By incorporating the effects of a magnetic field on charged ions of an element, Vauclair et al. (1979) have managed to explain Si abundance anomalies observed in a number of chemically peculiar magnetic stars and have demonstrated the important role played by horizontal magnetic field lines in the accumulation of silicon. Soon afterwards, Alecian & Vauclair (1981) – for silicon – and Michaud et al. (1981) – for several metals – have for the first time quantified, by means of a theoretical approach, the effect of the magnetic field geometry on atomic diffusion in the atmospheres of magnetic ApBp stars.

More recently, Alecian & Stift (2010) and Stift & Alecian (2012) have modelled the bi-dimensional distributions of various chemical elements in magnetic atmospheres. Their computations were based on the numerical code CARATSTRAT which evaluates the radiative accelerations of a number of metals by detailed opacity sampling, taking into account Zeeman desaturation, and solving the polarised radiative transfer equation. Equilibrium abundance stratifications due to atomic diffusion (they depend on magnetic field strength and inclination) are derived in an iterative procedure. These bi-dimensional

* E-mail: georges.alecian@obspm.fr

results make it possible to guess the horizontal and vertical abundance distributions to be found in stars with a given magnetic geometry, in the simplest case assumed to correspond to an oblique rotator with a centred dipole.

These theoretical predictions can be (and sometimes have been) confronted with empirical abundance maps derived with the help of (Zeeman) Doppler mapping (ZDM) (see Vogt et al. 1987). As a rule, these comparisons have either been inconclusive or have not resulted in agreement between predictions from theory and the detailed surface abundance distributions of a given star (see for instance Silvester et al. 2014). It is clear that current modelling not only of atomic diffusion but of ZDM as well must have their respective limitations. In this paper, we will discuss only the limitations in theoretical modelling. An improved grid of equilibrium abundance distributions of 16 chemical elements that result from the standard theoretical diffusion model is presented in Sec. 2. We then discuss in Sec. 3 extensions to the standard model that may be encountered in real stars, providing possible explanations for substantial deviations from observational predictions based on the standard model.

2 EQUILIBRIUM ABUNDANCE STRATIFICATIONS

Theoretical atmospheric models which take into account chemical stratifications due to atomic diffusion and which are based on extensive calculations of radiative accelerations have first been proposed by Alecian & Stift (2007) and by LeBlanc et al. (2009). In a later article, Alecian & Stift (2010) established bi-dimensional distributions of elements in magnetic atmospheres, assuming a dipolar geometry for the magnetic fields; variations in (vertical) abundance stratifications along the magnetic meridian – from the magnetic pole to the equator – were presented for 16 metals. The results discussed in the above-mentioned articles are all based on so called *equilibrium* stratifications representing the abundance stratifications necessary to have zero diffusion velocity for each element (remember that, at least in optically thick layers, the diffusion velocity largely depends on the local abundance of the element). This is approximately equivalent to the module of the radiative acceleration vector being equal to the module of the vector of gravity (the vectors are of opposite sign¹).

Our criterion for equilibrium thus consists in achieving an effective total acceleration (as defined by Eq. 15 of Alecian & Stift 2006) $g_{\text{tot}}^{\text{eff}} = 0$ for each element by means of an iterative modification of element stratifications. Let us emphasise the fact that an *equilibrium* calculation yields the maximum abundance of an element that can be supported by the radiation field in a given atmospheric layer. Therefore the equilibrium stratification cannot be considered to correspond to the one that would be obtained through the regular physical process of stratification build-up which obeys the

time-dependent continuity equation. Time-dependent solutions vs. equilibrium stratifications will be discussed in a forthcoming paper.

2.1 New calculations for a $T_{\text{eff}} = 10\,000\text{ K}$ atmosphere

The results of Alecian & Stift (2010) have been obtained with fixed atmospheric models based on solar abundances of the chemical elements. More recently, Stift & Alecian (2012) developed a modified CARATSTRAT code which ensures self-consistency in the calculation of equilibrium stratifications; the final vertical abundance distributions are now consistent with the stratified atmospheric structure computed with ATLAS12 (Kurucz 2005, Bischof 2005).

In Fig. 1 we present the equilibrium stratifications for 16 elements (adopting a main sequence atmospheric model with $T_{\text{eff}} = 10\,000\text{ K}$), obtained with this new self-consistent version of CARATSTRAT. The red dashed curves show the equilibrium stratifications in the presence of vertical magnetic lines of 20 kG (hereinafter considered as the magnetic pole of the stellar dipole), the red solid curves pertain to horizontal magnetic lines of 10 kG (corresponding to the magnetic equator of the same dipole). The black curves display the results for intermediate magnetic angles (60° and 80°) for which we have used available calculations for a grid of models (not restricted to a centred dipole geometry) with a field strength of 10 kG. For a dipole, the exact field strengths at these angles would actually be 11.1 kG and 10.1 kG respectively; the field strength of 10 kG for both 60° and 80° however is close enough to the exact ones for our present purpose. These 4 curves will hopefully help the reader to understand the predicted chemical stratifications as a function of the field geometry in the atmosphere of a star with a strong magnetic field. Comparison between the red dashed curves and the red solid ones reveals the abundance differences between the magnetic pole and the magnetic equator in the case of a dipolar magnetic field. Comparing the red curves to the black ones gives an indication as to the expected abundance contrast over the stellar surface. The arrows flag the layers for which convergence towards equilibrium has not been fully achieved (our criterion is $|\log(g_{\text{rad}}/g)| > 0.1$). These arrows point in the direction the curves should move to – by about 0.3 dex or more – in order to reach equilibrium, assuming that the behaviour of the radiative accelerations corresponds to the optically thick case (which however is not necessarily the case in optically thin layers). Generally, satisfactory convergence has been obtained for all inclinations² of magnetic lines less than 80° , but it turns out especially difficult to obtain convergence for 90° . This explains why the arrows are only shown for horizontal magnetic lines.

We have identified several numerical reasons why equilibrium is not attained:

- (i) Optically thin layers can suffer from screening of

¹ Theoretical considerations show that these vectors could point in the same direction only in a very particular and scarce case of a radiative acceleration dominated by some free-free transitions (Massacrier 2005).

² In Fig. 1, Mg, Si, Cu, Hg have not perfectly converged for 80° and $\log \tau < -3.0$. Notice that in our model, Mg and Ca are never supported by the radiative acceleration in layers deeper than $\log \tau \approx 1.0$, therefore, equilibrium cannot be reached for physical reasons.

the radiation field by underlying layers. When the concentration of a given element becomes very strong in layers at $\log \tau \approx -3.0$ for instance, photons originating from hotter deep layers are screened by the saturated lines of this element. Even if they are re-emitted, they are not necessarily re-emitted at the same temperature. This effect has well been identified in time-dependent diffusion calculations (see Alecian et al. 2011), but ideally it should not affect the search for equilibrium stratifications. However, our convergence algorithm appears sensitive to it because each iteration is subdivided into two sub-steps: in a first step a uniform increase of abundance is imposed on all layers, allowing us to determine how the medium reacts; in a second step the new abundance is determined by extra/interpolation. Screening may appear in the first sub-step, and so it impacts on the second sub-step. Most of the cases (arrows) shown in Fig. 1 are due this effect.

(ii) In some layers, diffusion coefficients of ionised particles across horizontal magnetic lines become very small as the proton density decreases. Since diffusion coefficients enter the expression of effective total acceleration (see Sec. 5.1 of Alecian & Stift 2006), vanishing coefficients become numerically very demanding on the convergence procedure (especially in the optically thin case), either because of numerical instabilities or because of an excessive increase in CPU time.

(iii) Another source of numerical instability consists in the difficulty experienced by the ATLAS12 module to deal with extremely strong abundance gradients which cause temperature inversions, or with very high over-abundances of metals. In some cases the equilibrium stratification may correspond to metal abundances comparable to the abundance of hydrogen, which is clearly unsupported by the code. For that reason we have put an upper limit of 9.5 (on a scale where $[H] = 12.00$) to metal abundances and we forbid a negative photon flux.

2.2 Results

Despite the above mentioned convergence problems, we consider the results shown in Fig. 1 entirely adequate for a discussion of the main abundance trends predicted by present-day theoretical models of magnetic ApBp stars. Stratifications have been derived for the same elements as those considered in Alecian & Stift (2010). In contrast to this earlier work, the atmospheric model with $T_{\text{eff}} = 10\,000$ K and $\log g = 4.0$ has been updated at every iteration step according to the abundance changes (see details in Stift & Alecian 2012).

The following discussion of the distributions of the different chemical elements assumes that equilibrium stratifications can actually be reached in real atmospheres and that NLTE conditions do not have a large effect on radiative accelerations (see a discussion of the limits of these assumptions in Sec. 3). Please note that our results are rather sensitive to the effective temperature and to the gravity (as a balance term against radiative acceleration), but also to a lesser degree to the strength of the magnetic field (due to Zeeman desaturation). They cannot therefore be generalised to all ApBp stars and must be used with extreme caution when confronting them with observations. Also keep in mind that a simple dipolar geometry is assumed through-

out even though detailed magnetic mapping of ApBp stars appear to reveal much more complex magnetic geometries. Hereinafter, we shall use the word *stratification* for vertical abundance inhomogeneities, the word *distribution* for horizontal ones. We use the word *cloud* for both stratification and distribution when abundance inhomogeneities reach a well discernible contrast.

Mg: Magnesium is deficient everywhere in the atmosphere except for $\log \tau < -2$ when magnetic lines are close to horizontal (inclination of lines $> 80^\circ$). High altitude clouds may be expected with high contrast (+2 dex) in zones with horizontal field lines. These clouds will manifest themselves as a ring/belt around the star (along the magnetic equator). Notice that Mg III (noble gas configuration with weak radiative acceleration) is the dominant ion in layers deeper than $\log \tau \approx 0$, so Mg is not supported in the deep atmosphere.

Al: Aluminium should form a cloud-like narrow ring/belt around the star (along the magnetic equator) located at $\log \tau \approx -3$. A horizontal magnetic field prevents Al ions from sinking, so the cloud is supported by the radiative acceleration of the neutral state (the same effect as invoked for silicon, see below). Al is expected to be strongly stratified because it is not supported by the radiation field around $\log \tau \approx -1.5$ where it becomes strongly deficient (the radiative acceleration is very weak for Al II).

Si: Silicon at solar abundance is not supported by the radiation field except when the magnetic field is almost horizontal. This strong dependence on the inclination of the magnetic field lines is consistent with previous predictions (Vauclair et al. 1979; Alecian & Vauclair 1981). However, the total radiative acceleration on Si is not large enough in our computations to explain the over-abundances observed in ApSi stars. This problem has been pointed out in the past by Michaud (1970) who proposed that auto-ionisation lines could play an important role. Alecian & Vauclair (1981) evaluated the importance of the Si II auto-ionisation lines but the atomic data available in the 1980's (Artru et al. 1981) did not allow to conclude positively on their role. The question still remains open since CARATSTRAT does not consider these particular transitions.

P: Phosphorus is well supported by the radiation field throughout the atmosphere. Its equilibrium abundance lies about 1 dex above the solar abundance with a rather smooth abundance stratification and a fairly uniform distribution. It does not appear to be very sensitive to the magnetic field. This is due to the rather high ionisation potential of P I (10.49 eV) which leads (for $-4.0 < \log \tau < 0.0$) to a significantly larger relative population of the neutral state than in the 15 other elements of our sample (except Hg). Let us point out that the equilibrium is hardly affected at all by the magnetic field because of the field-independence of the diffusion coefficient of the neutral state. This effect is further enhanced by the fact that the P II atomic lines are saturated (in contrast to those of Hg II), thus the weight of P I in the total radiative acceleration is large.

Ca: Calcium is not strongly supported by the radiation field

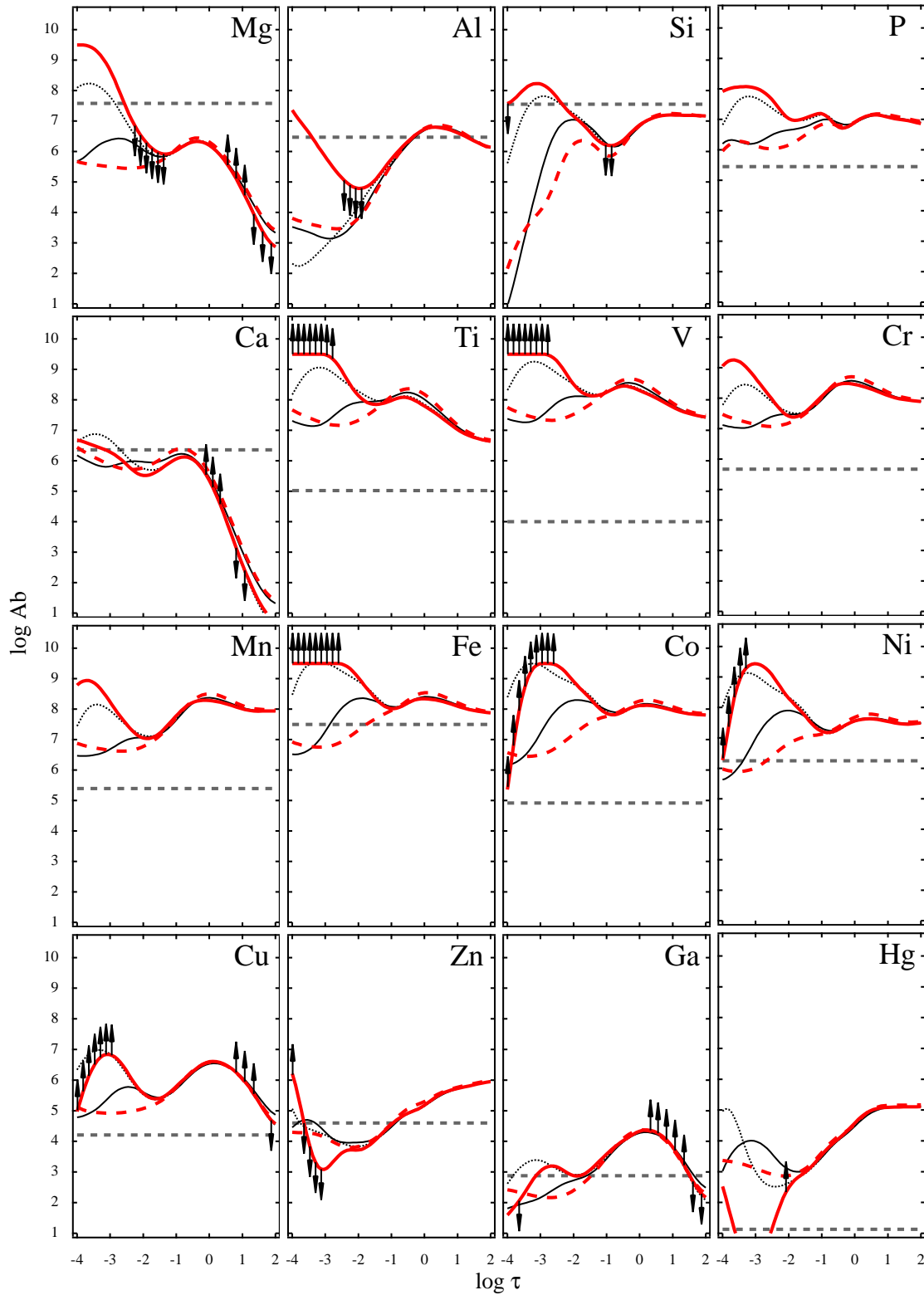


Figure 1. Logarithm of equilibrium abundances (given relative to hydrogen with $\log H = 12$) vs. logarithm of the optical depth (at 5000 \AA) for 16 elements. The model atmosphere is characterised by $T_{\text{eff}} = 10\,000 \text{ K}$ and $\log g = 4.0$. The horizontal grey heavy dashed line depicts the solar abundance (uniform), the red heavy dashed line shows the abundance stratification at the magnetic pole (20 kG, 0°), the red heavy solid line pertains to the magnetic equator (10 kG, 90°). The other curves correspond to intermediate magnetic parameters: the black solid line to 10 kG, 60° , the black dotted one to 10 kG, 80° . The arrows attached to the 90° curves indicate the layers where equilibrium has not been reached (see text).

because the dominant ion is Ca III in all layers of the atmosphere. Ca III exhibits a noble gas configuration with ensuing very small radiative acceleration. As a consequence, Ca has to be under-abundant everywhere to satisfy the equilibrium condition. Ca is atypical because for the other elements we find that the dominant ion (in layers $-4.0 < \log \tau < 0.0$) is generally the first ionisation state. The equilibrium stratification of Ca was calculated for the same effective temperature as the one adopted by Borsenberger et al. (1981) who took NLTE effects into account, but no magnetic field. Our results are quite close to theirs, regarding the position of the two abundance maxima. However, since their model atmosphere was computed assuming homogeneous solar abundances for all elements, we cannot compare the details of the respective Ca stratifications.

Ti and **V**: Titanium and vanadium display very similar equilibrium stratifications/distributions (the respective ionisation potentials of their first three ionisation states differ little). These elements should be over-abundant throughout the atmosphere with the largest enhancement taking the form of a moderately narrow ($\approx \pm 10^\circ$) ring/belt around the star (along the magnetic equator) above $\log \tau \approx -2$.

Cr and **Mn**: Chromium and manganese are also well supported by the radiation field, since an over-abundance of about 2 dex is needed before radiative acceleration balances gravity, even near the magnetic pole. We note that Cr and Mn could accumulate by up to 4 dex with respect to the solar value above $\log \tau \approx -2$ in a rather narrow belt/ring along the magnetic equator. Let us point out that these values are consistent with early calculations for Mn in the non-magnetic case (Alecian & Michaud 1981) and with observations (see Fig. 9 of Smith & Dworetzky 1993).

Fe: A high abundance of iron is well supported over the entire stellar surface. However, because of the high solar iron abundance, the lines are already highly saturated even before any stratification build-up due to atomic diffusion. Therefore, saturation effects on the radiative acceleration are fully effective at the very beginning of the modelling procedure and equilibrium is reached after only a few iterations for $\log \tau > -1.0$. This however is not the case in optically thin layers where the magnetic field may lead to a large ($> \pm 10^\circ$) over-abundant ring/belt around the magnetic equator. In the polar region, Fe can be under-abundant in upper atmospheric layers. Notice that inside the ring/belt, the abundance of iron attains the upper limit of $[\text{Fe}] = 9.5$ (with $[\text{H}] = 12.00$) we have fixed.

Co and **Ni**: Cobalt and nickel are less abundant in the upper layers of magnetic polar regions than in deep atmospheric layers ($\log \tau > -1.0$) where they could be uniformly strongly over-abundant. However, far from the polar regions (field angle $> 60^\circ$), Co and Ni accumulate and should form a large belt above $\log \tau \approx -2.0$ ($> \pm 30^\circ$) around the equator.

Cu: Copper shows a strong enhancement of its abundance (by about 2.5 dex) around $\log \tau = 0$, uniformly distributed over the stellar surface and not depending on the magnetic field. However, a well contrasted equatorial ring/belt (3 dex) may form above $\log \tau \approx -2.5$.

Zn: Zinc is over-abundant uniformly in layers deeper than $\log \tau = 0$, and under-abundant uniformly in the interval $-2.5 < \log \tau < -0.5$. Far from the magnetic pole (field angle $> 60^\circ$), Zn forms a belt around the star. However, this accumulation occurs in high layers, just above the uniformly under-abundant region, so it is difficult to know what will dominate in the observed spectra (over- or under-abundance) and how this could possibly be diagnosed.

Ga: Gallium is uniformly over-abundant ($\approx +1.5$ dex) in layers $-1.0 < \log \tau < +0.1$, and slightly under-abundant (≈ -1.0 dex) above $\log \tau = -2.0$. The abundance seems to be marginally dependent on the magnetic field for layers deeper than $\log \tau = -3.0$. These results are consistent with the study of the Ga case in upper main-sequence chemically peculiar (CP) stars by Alecian & Artru (1987) (with and without a magnetic field). Notice that these authors predicted Ga over-abundances to increase with effective temperature in the range $10\,000\text{K} < T_{\text{eff}} < 15\,000\text{K}$.

Hg: Mercury is a very special element in the study of CP stars since it is found to be highly over-abundant in HgMn stars, but not especially enhanced in spectra of magnetic ApBp stars. In the present calculations, the equilibrium stratification of Hg exhibits a uniform over-abundance (larger than $\approx +3$ dex) in layers deeper than $\log \tau = -1.0$, and a kind of hole around $\log \tau = -3.0$. This hole is much more conspicuous near the magnetic equator. A cloud of Hg seems to form at the magnetic equator above $\log \tau = -4.0$. As far as Hg is concerned, the equilibrium stratification approach is unsatisfactory when it comes to an explanation of the dichotomy between magnetic and non-magnetic stars, despite the fact that a hole develops around $\log \tau = -3.0$ in the presence of horizontal magnetic field lines. One should keep in mind the detailed study of Hg radiative accelerations by Proffitt et al. (1999) which has shown that Hg is strongly affected by non-LTE effects. Therefore, Hg should be considered in a time-dependent diffusion and possibly non-LTE framework.

3 BEYOND THE SIMPLEST THEORETICAL MODEL

The results discussed in previous section should be considered as an attempt to establish a kind of reference frame for abundance stratifications in a $T_{\text{eff}} = 10\,000$ K, $\log g = 4.0$ star with a dipolar magnetic field. The stratifications represent equilibrium values which are obtained through an iterative procedure. Since atomic diffusion is a process very sensitive to stellar properties, but also to any kind of perturbation, real stars could easily not conform to this simple model. In the following we shall shortly discuss several complications which can lead to deviations from the abundance stratifications obtained with the simple model.

3.1 NLTE effects

The role of NLTE effects has a particular status among the processes we consider in this section. In contrast to the processes enumerated below, NLTE is not just another parameter to add to the model or to neglect. We know that

above a certain depth in the atmosphere – which depends on the element – NLTE effects will be important enough to invalidate the results computed with the LTE based CARAT-STRAT code. So far, for 3 of the elements discussed in Sec. 2.2 there exist studies dealing with NLTE effects on their radiative accelerations. Borsenberger et al. (1981) looked at Ca, Alecian & Michaud (1981) at Mn. The paper on Hg by Proffitt et al. (1999) constitutes the most detailed modelling attempt ever of Hg radiative accelerations. It has been established that for the HgMn star χ Lupi, the observed abundance of mercury cannot be supported by the radiation field if NLTE effects are properly taken into account. Note that their calculations were done assuming a homogeneous overabundance of Hg. In the case of Ca and Hg, NLTE calculations have revealed that radiative accelerations within the framework of LTE are strongly overestimated in higher atmospheric layers. Therefore, one should consider calculations of LTE based radiative accelerations in upper atmospheric layers with the utmost caution. It is for this reason that the results shown in Fig. 1 are plotted only for layers with $\log \tau > -4.0$.

3.2 Decentred dipole

The hypothesis of a magnetic geometry characterised by a centred dipole implies that the star must have symmetrical magnetic hemispheres. If however the dipole is displaced from the centre of the star (Landstreet 1970), the magnetic equator will no longer delimit 2 symmetrical hemispheres. The magnetic field could be much stronger at one pole (leading to significantly larger amplifications of radiative accelerations) than at the other pole. Asymmetric abundance distributions are often found in ApBp stars (see for instance, Silvester et al. 2014). If diffusion were affected solely by the magnetic field, such an asymmetry could only be explained by the dipole being off-centre or by more complex magnetic geometries.

3.3 Multipolar fields

Although it is generally agreed that the dominant geometry of fossil magnetic fields is dipolar, this does not exclude the existence of quadrupolar or octupolar components (Michaud et al. 1981). Thus the field lines will not strictly follow a dipolar axial symmetry. Since the diffusion velocity is very sensitive to small variations in the angle between field line and stellar surface when the field is close to horizontal, quadrupolar and octupolar components can be expected to affect abundance distributions such as to make them patchier than in a strictly dipolar situation, but also to create warped rings about the magnetic equator.

3.4 Anisotropic wind

The mass loss velocity, assuming conservation of mass flux inside the star, is found to vary with depth approximately as the inverse of mass density; the diffusion coefficient for a given ion also varies more or less the same way. For small mass loss rates we can neglect the wind velocity in the continuity equation, for large mass loss rates the diffusion becomes negligible, but in between, for an adequate mass loss

rate, both velocities can compete. Competition of atomic diffusion with a stellar wind (or with mass loss) has first been considered by Vauclair (1975) who invoked it to explain He-rich stars. Michaud et al. (1983) and Alecian (1996) included mass loss in the study of Am stars. Evolutionary models which take into account atomic diffusion, computed with the Montreal code (Vick et al. 2010) include mass loss among the standard competitors to atomic diffusion. Babel (1992) proposed a magnetically confined wind for 53 Cam, because he found that with atomic diffusion alone it was not possible to explain the observed abundance distributions in their entirety. The assumption of an anisotropic mass loss of about $3 \times 10^{-15} M_{\odot} \text{yr}^{-1}$ close to the magnetic pole significantly improved the consistency of the model with the observations available at that time.

Our results shown in Fig. 1 are parameter free, and thus assume zero mass loss velocity. It is clear that individual stars need to be modelled assuming non-zero mass loss velocity, in particular magnetic stars with confined anisotropic wind near the magnetic poles. Such an approach could certainly strongly modify the polar abundances shown in Fig. 1.

3.5 Mixing

In the modelling of ApBp stars (with and without magnetic fields), it is always assumed that the atmosphere is completely stable (note that in AmFm stars the atmospheres are convective, and so models including diffusion are restricted to internal layers). We will not develop here the arguments in favour of this universally accepted assumption; it can be justified from theoretical considerations, but empirical support comes from observational evidence – which has accumulated over recent years – for abundance stratifications. Still, one cannot completely rule out that weak mixing (including thermohaline convection, see Vauclair 2004) may take place, perhaps only over a few layers.

It is difficult to assess what happens in the atmosphere of a magnetic ApBp star with strong vertical stratifications depending on the angle between the field vector and the surface normal. If the local atmospheres were isolated, the horizontal element distributions would differ from layer to layer, and the local temperature structure would vary accordingly; electron density and gas pressure would not be the same for a given depth. Basic physics of course tell us that pressure equilibrium between the local atmospheres will be established on very short time-scales. Needless to say that nobody yet has pointed out this problem, even less addressed the question of how the stellar atmosphere manages to stay in equilibrium horizontally and vertically in the presence of such chemical inhomogeneities. Does this give rise to some large scale horizontal circulation (e.g. similar to a vortex), resulting in horizontal mixing?

3.6 Other processes

Keeping in mind that real stars will behave in a much more complex way than the various models, and knowing that atomic diffusion is easily perturbed, we have to realise that the list of physical processes which can modify the simple picture proposed in Fig. 1 is certainly larger than the enumeration given above.

Processes like accretion of diffuse matter or the infall of solid bodies need to be looked at. Accretion of gas/dust may be the preferred scenario to atomic diffusion for λ Boo type stars (see Turcotte & Charbonneau 1993), but not so for ApBp stars. Still, infall of solid bodies onto ApBp stars (including HgMn stars) may occasionally lead to a modification of the surface element distributions and abundances (Cowley 1977). The relaxation time – by atomic diffusion – of such events remains to be estimated; it will involve hydrodynamics and depend on diffusion times (which are different for each element).

Tidal effects may also be considered, especially for HgMn stars which are slightly more often found in double-lined spectroscopic binary systems than normal stars, frequently with eccentric orbits (Smith 1996). Even if tidal effects do not appear to lead to synchronisation of rotation for these binaries, they could possibly affect the stability of the atmosphere to a sufficient degree to cause detectable effects.

Among main-sequence CP stars, pulsations are found at least in roAp stars, and possibly in HgMn stars which partly share the region of slowly pulsating B type (SPB) stars in the HR-diagram (Alecian et al. 2009; Morel et al. 2014); for roAp stars, pulsations seem to coexist with vertical abundance stratifications (see for instance Freyhammer et al. 2009). It is not yet known how these pulsations interact with the atmospheric structure, and whether or not they induce weak mixing.

First however, prior to the exploration and incorporation into our models of any of the processes listed above, we have to keep in mind one of the main aspects of atomic diffusion which is not dealt with in this article: the time dependent nature of the build-up of chemical stratifications. This will be discussed in a forthcoming paper.

4 CONCLUSIONS

We have presented and discussed a comprehensive set of equilibrium stratifications of 16 chemical elements in the atmosphere of a magnetic star with $T_{\text{eff}} = 10\,000$ K and $\log g = 4.0$; field strengths of 10 and 20 kG were considered, with field lines inclined by 90° , 80° , 60° and 0° towards the surface normal. It emerges from these simulations that in the majority of cases, large over-abundances are found in higher atmospheric layers when the fields are almost horizontal. Given the sensitivity of the stratifications to the field angle, we expect very large over-abundances to show up mainly along and near the magnetic equator in upper atmospheric layers – some patchy structure may be due to slight deviations of the field direction from the surface normal – more moderate ones around the magnetic poles. We have emphasised the fact that these results strongly depend on the fundamental parameters of a star; they should thus not be extended indiscriminately to all kinds and classes of CP stars with their considerable range in effective temperature and gravity.

It must be admitted that at present this kind of modelling based on equilibrium calculations is far too simple. Besides the fact that equilibrium calculations do not incorporate the continuity equation, we have listed a number of physical processes (such as NLTE, multipolar fields, anisotropic wind, etc.) which can strongly affect the build-

up of abundance stratifications and which should be introduced into numerical codes dealing with atomic diffusion in atmospheres (including CARATSTRAT). The increase in the number of free parameters constitutes of course a drawback.

We think that time-dependent approach should be the most realistic approach, but it still needs further development (work is in progress). Notice also that time-dependent calculations are extremely sensitive both to boundary and initial conditions. Besides possible physical instabilities in optically thin cases (Alecian et al. 2011), these calculations are faced with numerical stability problems, viz. for layers where the magnetic field is horizontal. In contrast, whereas the modelling of equilibrium stratifications has attained a state of superior maturity, it can hardly ever be applied to a given real, observed atmosphere (except perhaps in places where the field is almost horizontal) because by definition it only gives the maximum abundance which can be supported by radiative acceleration. Still, it offers a reference frame within which general statistical abundance trends found in CP stars all along the main-sequence can be analysed and interpreted.

Concerning the apparent disagreement between theoretical predictions and recently published empirical maps, we think that it will be important to check the ability of ZDM algorithms to detect complex abundance structures, in particular those predicted by diffusion theory for simple configurations, such as for instance small spots and thin, possibly warped rings. It will also be necessary to verify the effects of inhomogeneous vertical and horizontal, field-dependent abundance distributions (including self-consistent models of atmospheres) on the inversion procedure. **Theoretical modelling on its side will have to consider more realistic magnetic structures such as those derived from observations.**

Despite appearances, the outlook is by no means bleak. Numerical modelling that includes atomic diffusion has made tremendous progress over recent years, establishing – among others – incontrovertibly the sensitivity to the inclination of the magnetic field lines in the build-up of vertical abundance structure. Long before the sophisticated calculations presently possible, equilibrium stratifications have predicted statistical trends in the abundance anomalies observed in CP stars, as for instance the dependence of the maximum Mn overabundance on the effective temperature in HgMn stars (confirmed by Smith & Dworetzky 1993). Time-dependent diffusion calculations (Alecian et al. 2011) have unveiled the complex behaviour of the build-up of abundance stratifications and have provided new insight into the physics of this process.

ACKNOWLEDGEMENTS

Most of the numerical results discussed in this paper have been obtained using the numerical code CARATSTRAT developed in collaboration and written mostly by M. J. Stift. Thanks also to him for constructive discussions in the framework of our longstanding collaboration. This work has been supported by the Programme National de Physique Stellaire (PNPS) of CNRS/INSU, and by Observatoire de Paris-Meudon in the framework of *Actions Fédératrices Etoiles*. This work was partly performed using HPC resources from

GENCI-CINES (grants c2014045021, c2015045021). Thanks go to AdaCore for providing the GNAT GPL Edition of its Ada2005 compiler.

This paper has been typeset from a \TeX / \LaTeX file prepared by the author.

REFERENCES

- Alecian G., 1996, *A&A*, 310, 872
- Alecian G., Artru M., 1987, *A&A*, 186, 223
- Alecian G., Gebran M., Auvergne M., Richard O., Samadi R., Weiss W. W., Baglin A., 2009, *A&A*, 506, 69
- Alecian G., Michaud G., 1981, *ApJ*, 245, 226
- Alecian G., Stift M. J., 2006, *A&A*, 454, 571
- Alecian G., Stift M. J., 2007, *A&A*, 475, 659
- Alecian G., Stift M. J., 2010, *A&A*, 516, A53+
- Alecian G., Stift M. J., Dorfi E. A., 2011, *MNRAS*, 418, 986
- Alecian G., Vauclair S., 1981, *A&A*, 101, 16
- Artru M. C., Praderie F., Jamar C., Petrini D., 1981, *A&A*, 96, 380
- Babcock H. W., 1949a, *The Observatory*, 69, 191
- Babcock H. W., 1949b, *PASP*, 61, 226
- Babcock H. W., 1958, *ApJ*, 128, 228
- Babcock H. W., Burd S., 1952, *ApJ*, 116, 8
- Babel J., 1992, *A&A*, 258, 449
- Bailey J. D., Landstreet J. D., Bagnulo S., 2014, *A&A*, 561, A147
- Bischof K. M., 2005, *Memorie della Societa Astronomica Italiana Supplementi*, 8, 64
- Borsenberger J., Praderie F., Michaud G., 1981, *ApJ*, 243, 533
- Cowley C. R., 1977, *Ap&SS*, 51, 349
- Deutsch A. J., 1956, *PASP*, 68, 92
- Freyhammer L. M., Kurtz D. W., Elkin V. G., Mathys G., Savanov I., Zima W., Shibahashi H., Sekiguchi K., 2009, *MNRAS*, 396, 325
- Khokhlova V. L., 1994, in Zverko J., Ziznovsky J., eds, *Chemically Peculiar and Magnetic Stars On the Comparison of Different Codes for CP Stars Surface Mapping*. p. 60
- Kurucz R. L., 2005, *Memorie della Societa Astronomica Italiana Supplementi*, 8, 14
- Landstreet J. D., 1970, *ApJ*, 159, 1001
- LeBlanc F., Monin D., Hui-Bon-Hoa A., Hauschildt P. H., 2009, *A&A*, 495, 937
- Massacrier G., 2005, in Alecian G., Richard O., Vauclair S., eds, *EAS Publications Series Vol. 17 of EAS Publications Series, Radiative accelerations through photoionization and bremsstrahlung; autoionization*. pp 61–66
- Michaud G., 1970, *ApJ*, 160, 641
- Michaud G., Charland Y., Megessier C., 1981, *A&A*, 103, 244
- Michaud G., Tarasick D., Charland Y., Pelletier C., 1983, *ApJ*, 269, 239
- Morel T., Briquet M., Auvergne M., Alecian G., Ghazaryan S., Niemczura E., Fossati L., Lehmann H., Hubrig S., Ulu-soy C., Damerdjy Y., Rainer M., Poretti E., Borsa F., Scardia M., et. al. 2014, *A&A*, 561, A35
- Proffitt C. R., Brage T., Leckrone D. S., Wahlgren G. M., Brandt J. C., Sansonetti C. J., Reader J., Johansson S. G., 1999, *ApJ*, 512, 942
- Ryabchikova T., 2008, *Contributions of the Astronomical Observatory Skalnaté Pleso*, 38, 257
- Silvester J., Kochukhov O., Wade G. A., 2014, *MNRAS*, 444, 1442
- Smith K. C., 1996, *Ap&SS*, 237, 77
- Smith K. C., Dworetsky M. M., 1993, *A&A*, 274, 335
- Stift M. J., Alecian G., 2012, *MNRAS*, 425, 2715
- Turcotte S., Charbonneau P., 1993, *ApJ*, 413, 376
- Vauclair S., 1975, *A&A*, 45, 233
- Vauclair S., 2004, in Zverko J., Ziznovsky J., Adelman S. J., Weiss W. W., eds, *The A-Star Puzzle Vol. 224 of IAU Symposium, Thermohaline convection and metallic fingers in polluted stars*. pp 161–166
- Vauclair S., Hardorp J., Peterson D. M., 1979, *ApJ*, 227, 526
- Vick M., Michaud G., Richer J., Richard O., 2010, *A&A*, 521, A62
- Vogt S. S., Penrod G. D., Hatzes A. P., 1987, *ApJ*, 321, 496